Chapter 6: Efforts toward single molecule fluorescence imaging of nAChRs

6.1 Abstract

Fluorescence studies probing conformational changes in nAChRs upon activation have the potential to bridge a wealth of functional data on these receptors from electrophysiology with emerging structural models for activation. Incorporation of fluorophores as unnatural amino acid side chains by nonsense suppression is an attractive option for selective labeling of these receptors for fluorescence studies. This chapter describes efforts to replicate and expand upon an earlier report from our group in which single nAChRs bearing a BODIPY fluorophore as an amino acid side chain were imaged in the membrane of *Xenopus laevis* oocytes. Progress was hampered by high levels of background fluorescence. Several approaches to circumvent this issue are described, including improved sample preparation, dye conjugation, and the use of a fluorescent tRNA with partially quenched fluorescence.

6.2 Introduction

Our understanding of nAChR gating motions lags far behind our functional understanding of these receptors from electrophysiology. Opening of the ion-conducting pore 60 Å away from the ligand binding site is thought to occur through closure of the C loop around the agonist and twisting of the entire extracellular domain coupled to tilting of TM2 and TM3.[1] Computational studies, x-ray crystallography of homologous bacterial channels, and cryo-EM structures of acetylcholine-bound and agonist-free

nAChRs corroborate some of these proposed gating motions. [2-6] However, many question remain: How large are the gating motions in the actual receptor? Are motions symmetric throughout the five subunits of the channel? What are the structures of desensitized and "uncoupled" states? Fluorescence studies on functional receptors in native cell membranes have the potential to address these questions.

To answer these sorts of detailed structural questions, small molecule fluorophores are highly preferred over fluorescent proteins due to their greater brightness, greater photostability, and most of all, small size. The tradeoff, of course, is the significant challenge of specific attachment of the fluorophore to the protein, especially *in vivo*. Incorporating the fluorophore as the side chain of an unnatural amino acid is an especially attractive option, and this approach has previously been used to incorporate single fluorophores into membrane proteins *in vivo*.[7,8] This approach obviates the need for the attachment site to be solvent accessible, and also ensures site-selective labeling.

Previously, the Dougherty and Lester labs reported the successful incorporation of a BODIPY fluorophore into the nAChR by nonsense suppression in *Xenopus* oocytes, and single molecule imaging of these fluorescent receptors.[9] The fluorophore used was BODIPYFL, which was conjugated to a lysine side chain (Figure 6.1A). This side chain was incorporated into the β19' site of the muscle-type nAChR, and the presence of functional receptors at the cell membrane was confirmed by electrophysiology. Fluorescence imaging was conducted on devitellinized oocytes using total internal reflection fluorescence (TIRF) microscopy. TIRF, in which only molecules less than ~100 nm from the glass surface the cell membrane is resting against are illuminated, was critical to enable fluorescent imaging at the membrane, given the high autofluorescence

of the oocyte interior[10] and a large excess of fluorescent tRNA-Lys-BODIPY injected into the cell.

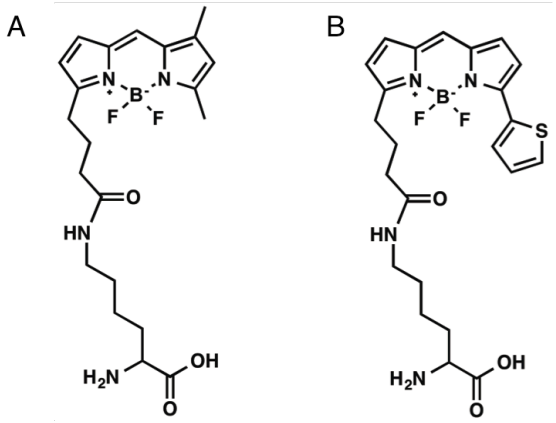

Figure 6.1. (A) Structure of Lys-BODIPYFL. **(B)** Structure of Lys-BODIPY558.

A logical extension of this work is the incorporation of two different fluorophores site-specifically into the nAChR to enable Förster resonance energy transfer (FRET) studies. A recently expanded toolkit of tRNAs for nonsense suppression in *Xenopus* oocytes enables the incorporation of multiple unnatural amino acids simultaneously.[11] Walrati Limapichat laid much of the groundwork for incorporation of multiple fluorophores into the nAChR, including the preparation of Lys-BODIPYFL and Lys-BODIPY558 (Figure 6.1) conjugated to dCA (which are used in the experiments described below), screening of sites for fluorophore incorporation, and preliminary imaging experiments.[12] These fluorophores have been incorporated into calmodulin as amino acid side chains by nonsense suppression *in vitro* and have a Förster radius (R_0) of 60Å.[13]

This work aims to optimize the expression and TIRF imaging of fluorescent amino acids in nAChRs *in vivo* to enable two-color FRET experiments. Progress was

hampered by high background from fluorescent tRNA injected into the cell. Efforts are described to minimize this fluorescence background, including different membrane preparations and the preparation of a tRNA-Lys-BODIPYFL with partially quenched fluorescence. Analysis of single puncta simultaneously at two wavelengths is also discussed.

6.3 Results and Discussion

6.3.1 Background fluorescence from tRNA-BODIPY

As a starting point, visualization of receptors bearing a single Lys-BODIPYFL was attempted, under similar conditions to those used by Pantoja and co-workers in our lab's earlier report on receptor single molecule imaging.[9] The β70 site was chosen for Lys-BODIPYFL incorporation, as this position is known to be permissive to the incorporation of large side chains.[14] The amber suppressor tRNA TQAS was chosen for these experiments, as it shows low levels of reacylation in *Xenopus* oocytes.[15] As a control, TQAS tRNA acylated with Lys-BODIPYFL (TQAS-BODIPYFL) was injected into cells alone to assess the level of background fluorescence from intracellular tRNA. High levels of fluorescence were seen for both β70 mRNA + TQAS-BODIPYFL and tRNA only conditions (Figure 6.2). Some cell-to-cell variability was seen for both conditions. Overall the two conditions were indistinguishable from each other, indicating that background fluorescence from tRNA-BODIPY was too high to permit visualization of fluorescent receptors. Conditions were not identical to those used by Pantoja[9], but differences are not expected to affect the background fluorescence levels (conditions used here: 20 ng total of 2:5:1:1 α/β70TAG/γ/δ mRNA mix, 10 ng of TQAS-BODIPYFL

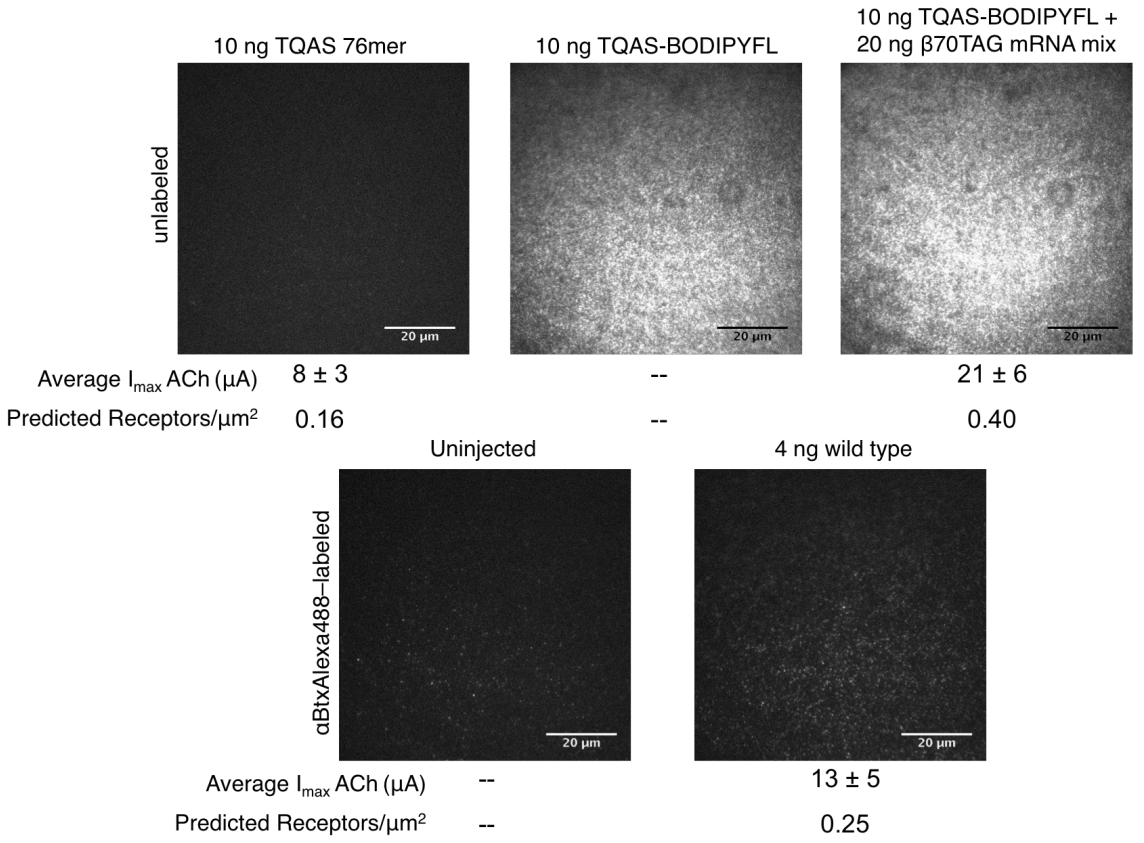

Figure 6.2. TIRF images and average whole cell currents from *Xenopus laevis* oocytes incubated for 24 hrs after the injection condition noted over each panel. Panels are representative images from the same cell batch that the electrophysiology recordings were made on. I_{max} values are for a saturating ACh concentration (1000 μM). Receptor density on the cell surface is predicted from macroscopic currents observed from that cell batch, using previously reported assumptions.[9] Brightness range for all panels is 100 counts (black) to 3000 counts (white).

tRNA, 24 hr incubation. Pantoja conditions: 25 ng total of 2:5:1:1 α/β19'GGGU/γ/δ mRNA mix, 12.5 ng of YFaFS$_{AAAC}$-Lys-BODIPYFL tRNA, 24 hr incubation). Subsequent imaging using the same tRNA employed by Pantoja (YFaFS$_{AAAC}$-Lys-BODIPYFL tRNA) gave similar background fluorescence levels.

The fluorescence observed has a relatively uniform, granular appearance (Figure 6.2) that is completely stationary, inconsistent with freely diffusing fluorophores within

the cytosol. We speculate that the fluorophores are most likely either embedded in the plasma membrane, with minimal lateral diffusion, or are adhered to the glass coverslip.

In the Pantoja and co-workers report, some background fluorescence was observed from cells injected with tRNA-BODIPYFL alone, but this was observed at significantly lower puncta densities than the mRNA + tRNA-BODIPYFL conditions ($0.007 \pm 0.002/\mu m^2$ for tRNA alone, compared with $0.021 \pm 0.003/\mu m^2$ for mRNA + tRNA).[9] The fluorescence observed in the images obtained here (tRNA only and tRNA + mRNA conditions) was too dense for individual puncta to be counted.

Surface expression of receptors incorporating Lys-BODIPYFL was confirmed by electrophysiology (Figure 6.2). High levels of reacylation and/or readthrough are seen for nonsense suppression at this site, as indicated by a control in which unacylated 76mer tRNA is injected in place of tRNA-Lys-BODIPYFL. Assuming a typical average plasma membrane surface area of an oocyte and uniform membrane adhesion to the glass coverslip under imaging conditions, and using the known single channel conductance for this receptor, receptor density on the plasma membrane can be estimated from whole cell current magnitudes.[9] These estimates (Figure 6.2) indicate that when currents from reacylation are subtracted, densities on the order of 0.2 receptors/μm^2 are expected for receptors bearing Lys-BODIPYFL under these conditions. While Pantoja only observed puncta at ~1/3 the density predicted by whole-cell currents, the larger currents observed here should still yield greater puncta densities than the $0.021 \pm 0.003/\mu m^2$ observed by Pantoja, with approximately the same amount of tRNA injected. While our failure to distinguish between tRNA only and tRNA + mRNA images is apparently due to high

background fluorescence from tRNA, we are not experiencing uniquely low levels of receptor expression relative to the quantity of fluorescent tRNA injected.

A more sensitive CCD camera was used for these experiments than in the Pantoja study, leading us to wonder whether the higher background fluorescence levels we observed were simply due to greater camera sensitivity, such that brighter punctate features were not visible over the high background observed. However, no new image features emerged (punctate or otherwise) when imaging at lower excitation laser intensities or shorter image integration times: we simply obtained dimmer images with the same uniform granular fluorescence pattern. To help reference the fluorescence intensities we observed, we labeled cells expressing wild type receptors with Alexa488-labeled α-bungarotoxin (αBtxAlexa488, from Life Technologies). This conjugate has approximately one dye per α-bungarotoxin molecule[9], and there are two α-bungarotoxin binding sites per receptor. Alexa488 has a similar fluorescence emission profile as BODIPYFL and was reported to have approximately three times the brightness of BODIPYFL when each dye was conjugated to streptavidin.[16] Some punctate αBtxAlexa488 background labeling was seen on uninjected cells (Figure 6.2), but more punctate fluorescence was seen for labeled cells expressing wild type receptors (Figure 6.2). These puncta are dimmer than the fluorescence background seen in cells injected with tRNA-Lys-BODIPYFL, indicating that imaging fluorescent receptors against this background will not be possible.

We wondered if optimizing the amount of mRNA and tRNA injected might yield conditions under which fluorescent receptors could be resolved above the background. As expected, the level of background fluorescence is dependent on the amount of tRNA

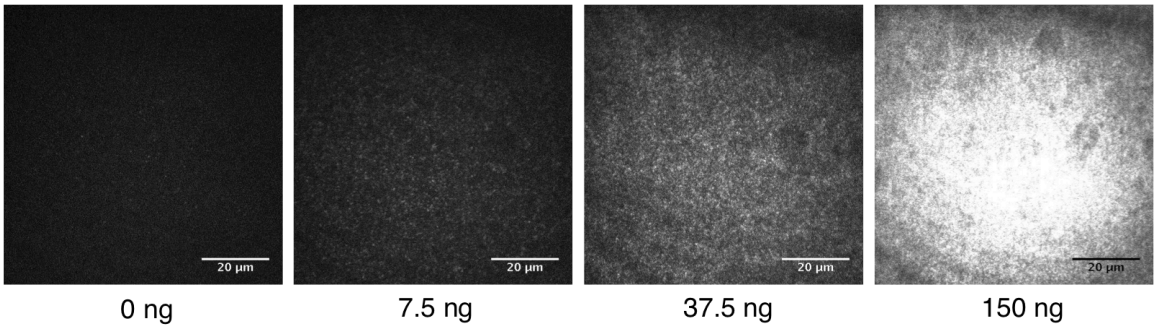

Figure 6.3. TIRF images from oocytes injected with varying amounts of TQAS-BODIPYFL. Brightness range for all panels is 100 counts (black) to 1500 counts (white).

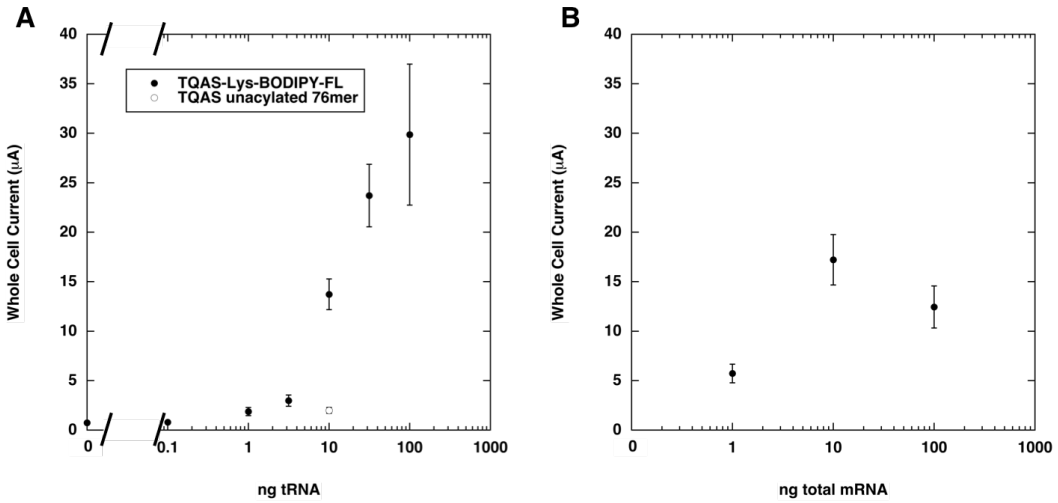

Figure 6.4. Whole cell currents from cells injected with various quantities of mRNA and tRNA. Incubation time is 24 hrs. **(A)** tRNA titration; all cells injected with 20 ng β70TAG mRNA mix and the indicated quantity of tRNA. **(B)** mRNA titration; all cells injected with 37.5 ng TQAS-BODIPYFL and the indicated quantity of β70TAG mRNA mix.

injected (Figure 6.3). Surface expression levels (judged by measuring whole-cell currents) increase when injecting 10 ng rather than 1 ng of mRNA, but do not get any larger with 100 ng of mRNA (Figure 6.4A). Expression levels continually increased over the entire range of tRNA injection amounts tested (Figure 6.4B). These data suggest that tRNA is the limiting factor for receptor expression, and unfortunately it must be supplied at an enormous excess: a rough estimate of surface expression levels from macroscopic currents suggest that 3 x 10^4 tRNA molecules were injected per receptor ultimately

present on the cell surface. This estimate is for 24 hrs after injection of 20 ng total β70TAG mRNA and 10 ng TQAS-BODIPYFL tRNA. Comparison of absorbance values at 260 nm (λ_{max} for RNA) and 510 nm (λ_{max} for BODIPYFL) on TQAS-BODIPYFL tRNA using known molar absorptivity values indicate a 1:3 molar ratio of BODIPYFL to tRNA. This confirms that there is not an excess of BODIPY fluorophores in the tRNA solution and is consistent with the presence of some unacylated tRNA in the TQAS-BODIPYFL solution.

We wondered whether the background fluorescence we observed was from free BODIPY fluorophores, from Lys-BODIPY that had hydrolyzed off of the tRNA, or from fluorophores still attached to tRNA. The free backbone amine of Lys-BODIPY on the tRNA was protected with an NVOC group to minimize hydrolysis of the amino acid from the tRNA during preparation and storage, and was photolyzed immediately prior to oocyte injection. We compared fluorescence from oocytes injected under standard conditions to injection of tRNA-Lys-BODIPYFL-NVOC (i.e., the NVOC group was not photolyzed prior to injection) (Figure 6.5). Fluorescence was comparable for both

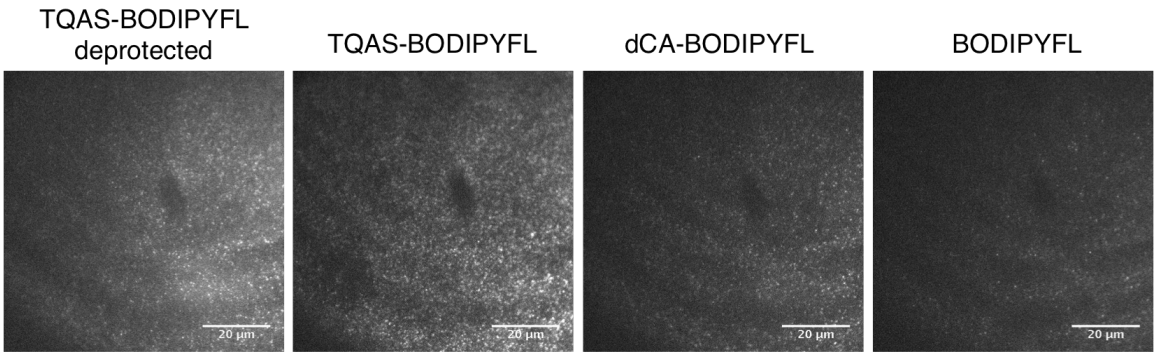

Figure 6.5. TIRF images from oocytes injected with various BODIPYFL species. All cells were injected with 0.1 pmol of the indicated species (= 2.5 ng TQAS-BODIPYFL). In the first panel TQAS-BODIPYFL was NVOC-deprotected by photolysis. All other samples were injected without photolysis. The common dark spot and interference pattern observed in all images is due to irregularities in the TIRF illumination field. Brightness range for all panels is 100 counts (black) to 3000 counts (white).

deprotected and NVOC-protected tRNA. We anticipate that much less of the Lys-BODIPYFL will hydrolyze from the tRNA in its NVOC-protected form, so background fluorescence from free Lys-BODIPYFL is not anticipated to be the issue.

To assess whether the nature of the moiety BODIPY is appended to changes the background signal, we also examined fluorescence from cells injected with the dinucleotide dCA appended to Lys-BODIPY (dCA-Lys-BODIPYFL-NVOC) and fluorescence from free BODIPYFL. Interestingly, somewhat less fluorescence was seen for dCA-BODIPY than for tRNA-BODIPY and less fluorescence still was seen for free BODIPY. It is possible that the hydrophobic BODIPY fluorophore partitions to the lipid-rich yolk of the oocyte unless tethered to a large hydrophilic moiety such as tRNA.

Cursory investigations using a different objective lens (100x, 1.65NA) and imaging on a different fluorescence microscope (Olympus IX81) also revealed similar images for tRNA-BODIPY only and for tRNA-BODIPY + mRNA conditions. These results suggest that optical issues (i.e., laser focusing, TIRF illumination, collection of fluorescence by the objective lens) were not likely to be the source of the background observed.

6.3.2 Optimization of vitelline membrane removal

Oocytes imaged by TIRF microscopy were first stripped of their vitelline membrane, a protein-rich layer of extracellular matrix surrounding the plasma membrane. Using a standard technique, this membrane was removed manually with forceps after osmotic shrinking of the oocyte. The plasma membrane of *Xenopus laevis* oocytes is heavily studded with microvilli extending through the extracellular matrix,[17] and previous

studies imaging devitellinized oocytes have suggested that the microvilli may be sheared during the standard manual devitellinization protocol.[18] We wondered whether the high fluorescent background observed could have been due to fluorophore leakage out of the oocyte via tears in the plasma membrane caused by devitellinization.

Other protocols have been reported for vitelline membrane removal that aim to preserve plasma membrane integrity. Two of these methods were investigated for their ability to reduce background fluorescence in this system. Both protocols were originally reported to improve the reliability of high-resistance seal formation for single channel patch clamp experiments. The first method aims to remove adhesions between the plasma membrane and vitelline membrane by enzymatic digestion.[19] For 60 min, cells are exposed to 4 mg/mL collagenase and 4 mg/mL hyaluronidase, after which cells are shrunk by exposure to hypertonic media. Upon shrinking, the vitelline membrane ("detached," though still intact) appears separated from the plasma membrane, while in the absence of enzymatic treatment the vitelline membrane wrinkles and shrinks together with the plasma membrane. This enzymatic treatment was conducted immediately prior to manual devitellinization and imaging.

In the second method, the vitelline membrane is completely digested enzymatically, so that manual stripping is unnecessary.[20] Digestion is achieved by protease treatment (0.05 mg/mL, Type VIII, Sigma) with gentle shaking. Swelling followed by disappearance of the vitelline membrane can be seen by light microscopy. While the literature report of this protocol cites complete digestion of the vitelline membrane within 3-4 min, we found that 30 min was required. To test whether membrane-expressed receptors are affected by the protease treatment, we performed

electrophysiology (2-electrode voltage clamp) immediately following digestion on oocytes expressing the wild-type muscle nAChR. We recorded an EC_{50} for ACh (17.4 ± 0.7 μM), only slightly shifted from untreated cells (23.2 ± 0.9 μM, from the same cell batch), and observed similar current magnitudes, suggesting that receptors are still functional.

These two devitellinization conditions were compared with standard manual devitellinization by imaging cells injected with the small organic dye fluorescein (1 pmol/oocyte – we inject approximately this molar quantity of tRNA per oocyte in standard experiments). Fluorescence from standard devitellinization conditions and the collagenase/hyaluronidase reduced adhesion method gave similar, moderate levels of fluorescence (Figure 6.6A, B). The protease devitellinization condition, however, gave

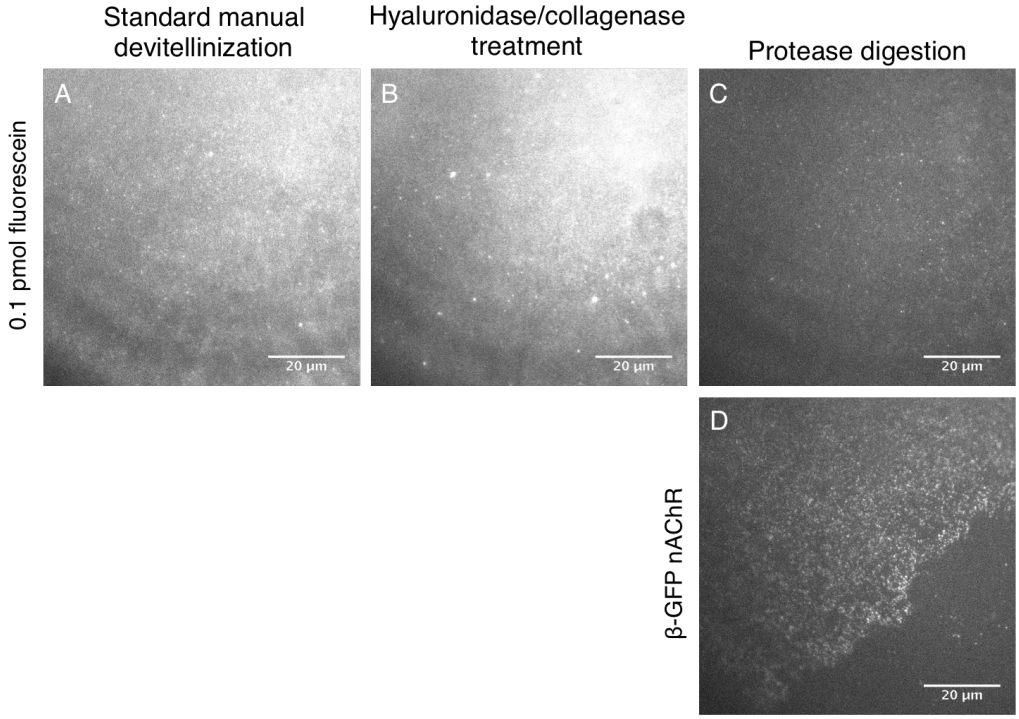

Figure 6.6. TIRF images from oocytes prepared under various devitellinization conditions. In top panels cells were injected with 0.1 pmol fluorescein and devitellinized by the method indicated. In the bottom panel the cell was injected with nAChR mRNA tagged with GFP on the β subunit. Brightness range for all panels is 100 counts (black) to 4000 counts (white).

very low fluorescence levels across many cells, consistent with less leakage of the dye from the oocyte (Figure 6.6C). To confirm that the plasma membrane was indeed exposed and adhered to the coverslip in the protease-digested cells, we imaged protease-treated cells expressing nAChRs with GFP appended to the β1 subunit (Figure 6.6D). Indeed, we observed patches of fluorescence from these cells. Of note, inspection in brightfield mode (data not shown) suggested that these crisply delineated bright patches likely correspond with adhered sections of membrane.

With respect to delineated regions of fluorescence, the opposite result was observed in images from select oocytes prepared either by standard manual devitellinization or hyaluronidase/collagenase treatment prior to manual stripping. In isolated cases, regions where the plasma membrane did not appear tightly adhered to the glass coverslip (by inspection in brightfield mode) had higher fluorescence levels than adjacent regions that appeared to be adhered (Figure 6.7). The inverse is expected for TIRF imaging of the membrane, as only fluorophores within ~100 nm of the coverslip

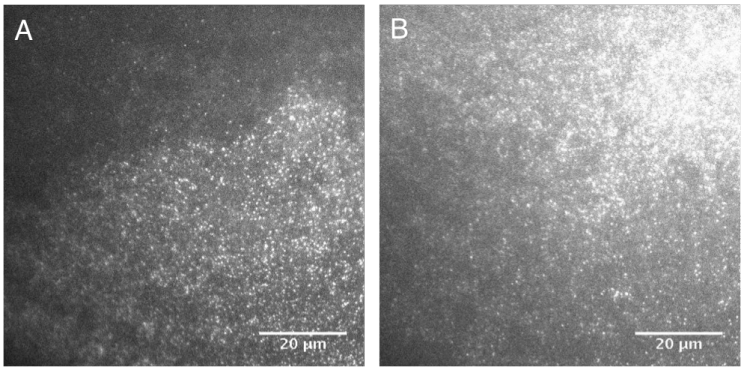

Figure 6.7. TIRF images from oocytes injected with 10 ng TQAS-BODIPYFL and 10 ng α70TAG mRNA mix, imaged at apparent boundaries of plasma membrane adhesion to the glass coverslip. Adhesion to the coverslip is inferred from inspection under bright field illumination (not shown). **(A)** Oocyte devitellinized manually after hyaluronidase/collagenase treatment. Top of this field (dark region) appears adhered to the coverslip, while the bottom (brighter region) does not. **(B)** Oocyte devitellinized by standard manual technique without enzymatic treatment. Bottom of this field (darker region) appears adhered to the coverslip, while the top (brighter region) does not. Brightness range for both panels is 100 counts (black) to 4000 counts (white).

surface will be illuminated. This could be consistent with leakage of fluorophores from the cytosol into the space between the coverslip and plasma membrane, whereas diffusion of fluorophores into adhered regions is more restricted.

The protease condition seems promising for reducing background fluorescence. However, when imaging protease-treated cells injected with tRNA-BODIPY alone or with tRNA-BODIPY + mRNA, no difference was observed; both yielded comparable levels of punctate fluorescence (Figure 6.8), albeit with lower levels of background fluorescence than in earlier attempts (i.e., Figure 6.2).

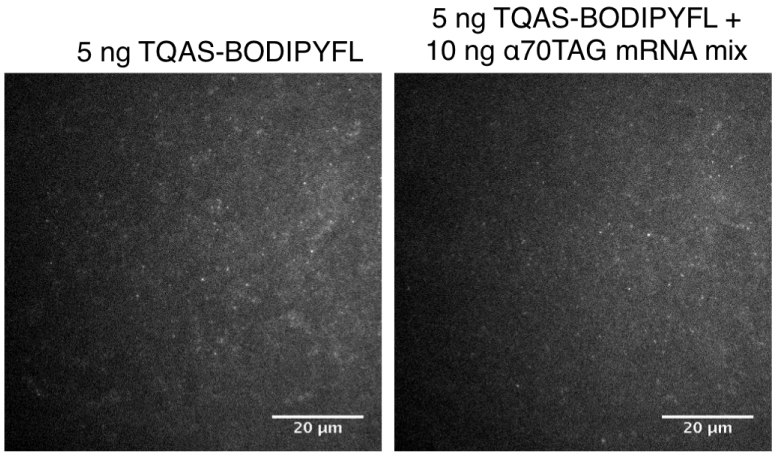

Figure 6.8. TIRF images from cells subjected to protease devitellinization conditions. Injection conditions are indicated above panels. Brightness range for both panels is 500 counts (black) to 3000 counts (white).

It should be noted that after significant practice at the standard technique using forceps to manually strip the vitelline membrane, low background fluorescence levels were sometimes obtained (Figure 6.9) – roughly at the same low background fluorescence levels seen in the protease digestion experiments. Good oocyte health may also be critical for this result, though this was not investigated systematically. With extremely precise technique, it is plausible that this method could yield satisfactorily low

levels of fluorescence, as were evidently obtained in the Pantoja et al. study.[9] However, even at the low background fluorescence levels sometimes obtained in the experiments described here, no difference was ever observed between tRNA only and tRNA + mRNA conditions, as the Pantoja study describes.

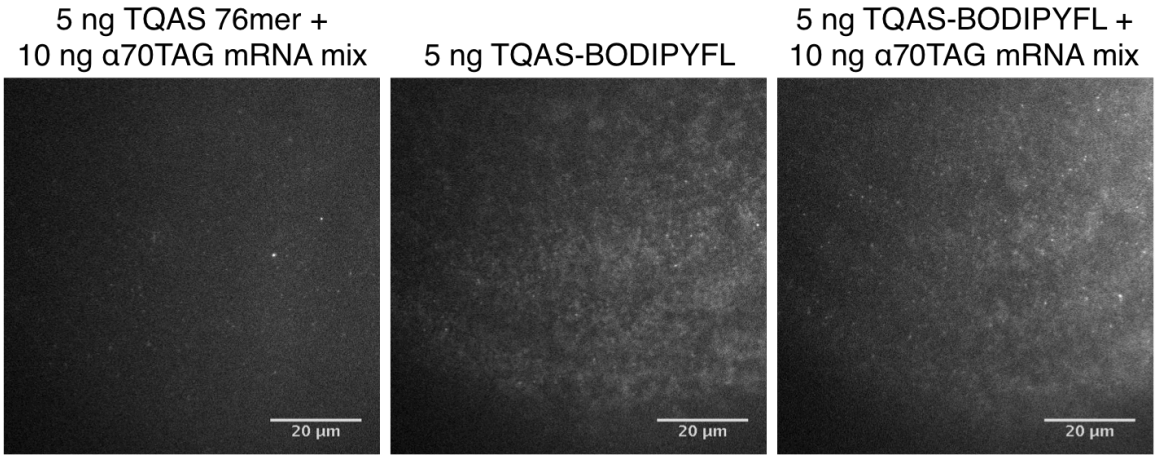

Figure 6.9. TIRF images showing low background from standard manual devitellinization conditions. Injection conditions are indicated above panels. Brightness range for all panels is 250 counts (black) to 3500 counts (white).

6.3.3 Two-color imaging and single puncta analysis

As receptors could not be convincingly visualized above fluorescent background in the single color imaging experiments described above, we turned to two-color FRET imaging. FRET should allow a means to distinguish receptors from background as it should only be observed from receptors bearing two fluorophores. In these experiments, we used Alexa488-labeled α-bungarotoxin to label receptors with this donor fluorophore, which could be excited by the same 488 nm laser used for the BODIPYFL experiments. The acceptor fluorophore used was BODIPY558 (Figure 6.1), incorporated as a Lys-BODIPY558 side chain at the γ70 site. Here we used the opal suppressor tRNA TQOpS'.[15,21] In these experiments, oocytes expressing γ70Lys-BODIPY558 are labeled

with Alexa488-α-bungarotoxin immediately prior to imaging. It should be noted that there are two α-bungarotoxin binding sites on the muscle-type nAChR: at α/γ and α/δ interfaces. This leads to a complex FRET scenario with the potential for two donor fluorophores and a single acceptor. Based on rough modeling from the torpedo nAChR structure,[22] these two donor-acceptor distances are expected to be roughly 40 Å and 60 Å. However, only 74% of α-bungarotoxin molecules are reported to be Alexa488-labeled in the supplied conjugate, and some of these donor fluorophores are likely bleached during sample handling and focus, such that 48% of Alexa488-α-bungarotoxin labeled receptors are reported to give only a single photobleaching step under similar conditions to those used here.[9] Hence, some receptors will be expected to have two Alexa488 donor fluorophores, while many should have only one.

Two-color imaging is enabled by use of the OptoSplit II image splitter, which allows side-by-side imaging of the same field at two wavelengths. Excitation is identical to the experiments described above: a 488 nm laser is used to excite donor fluorophores. The fluorescence emission light path is split by a dichroic mirror and the two resulting light paths transit different bandpass filters, allowing for selection of the donor and acceptor emission wavelengths of interest, which are projected side-by-side onto the camera.

Corresponding puncta in the two channels were identified using IDL scripts written by Taekjip Ha's lab at the University of Illinois (details in Methods section), allowing the intensity of a given punctum in both channels to be determined as a function of time. Puncta with step-like fluorescence intensities were considered for further analysis. For all conditions, cells were labeled with Alexa488-α-bungarotoxin. For a

control in which cells are injected with γ70TGA mRNA and unacylated 76mer tRNA, fluorescence in the donor channel is generally consistent with single step photobleaching, with little or no fluorescence in the corresponding acceptor channel (Figure 6.10). These donor fluorophores are likely the result of both nonspecific labeling of Alexa488-α-bungarotoxin and of labeling "background" receptors generated from nonsense suppression by tRNA acylated *in vivo*.

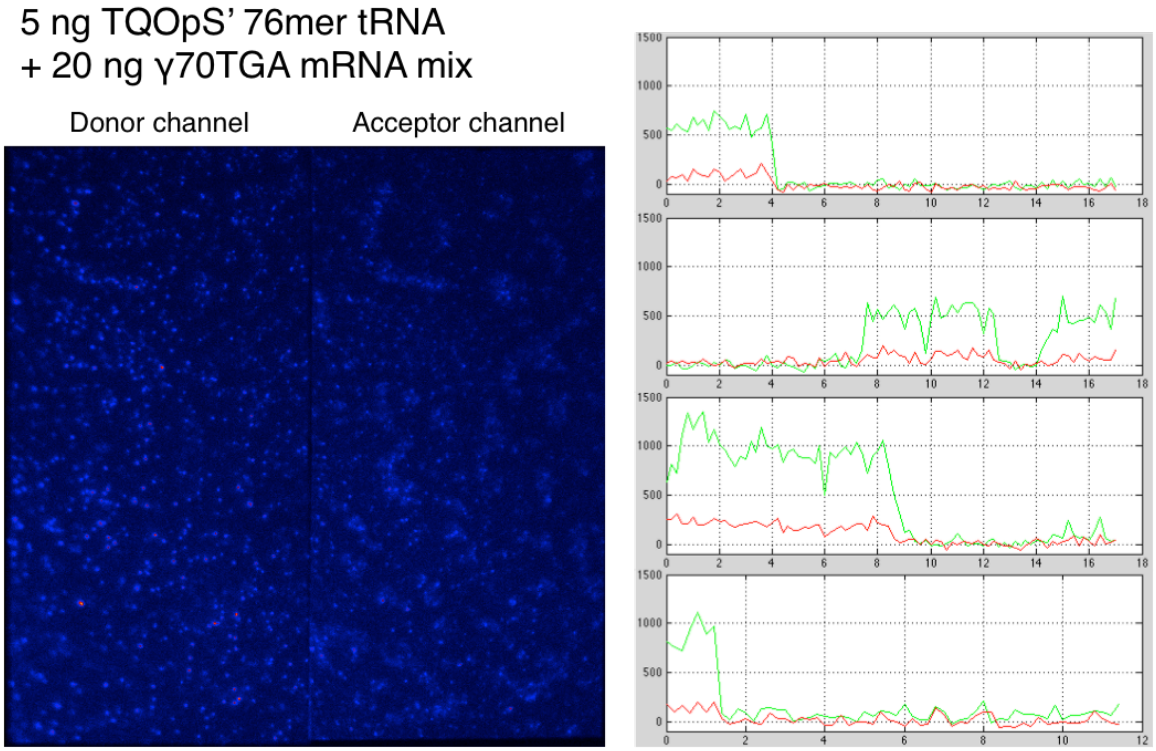

Figure 6.10. Two-color fluorescence image and fluorescence traces from selected puncta of a cell injected with unacylated TQOpS' 76mer tRNA and labeled with αBtxAlexa488. Entire fluorescence image is shown with the same "heatmap" false-color scheme. Donor channel and acceptor channel represent the same field of view imaged at different emission wavelengths. Fluorescence traces show donor channel intensity (green) and acceptor intensity (red) for the same punctum. Horizontal axis is time (s) and vertical axis is intensity (counts). Note the small degree of spectral bleedthough of donor fluorescence into the acceptor channel (visible in both images and in traces).

Cells injected with γ70TGA mRNA and tRNA-BODIPY558 do have puncta with fluorescence in both donor and acceptor channels, as would be expected for FRET (Figure 6.11). No clear hallmarks of single molecule FRET were observed however, such as anticorrelated donor and acceptor fluorescence intensities – specifically a jump in donor fluorescence intensity upon acceptor blinking or bleaching.

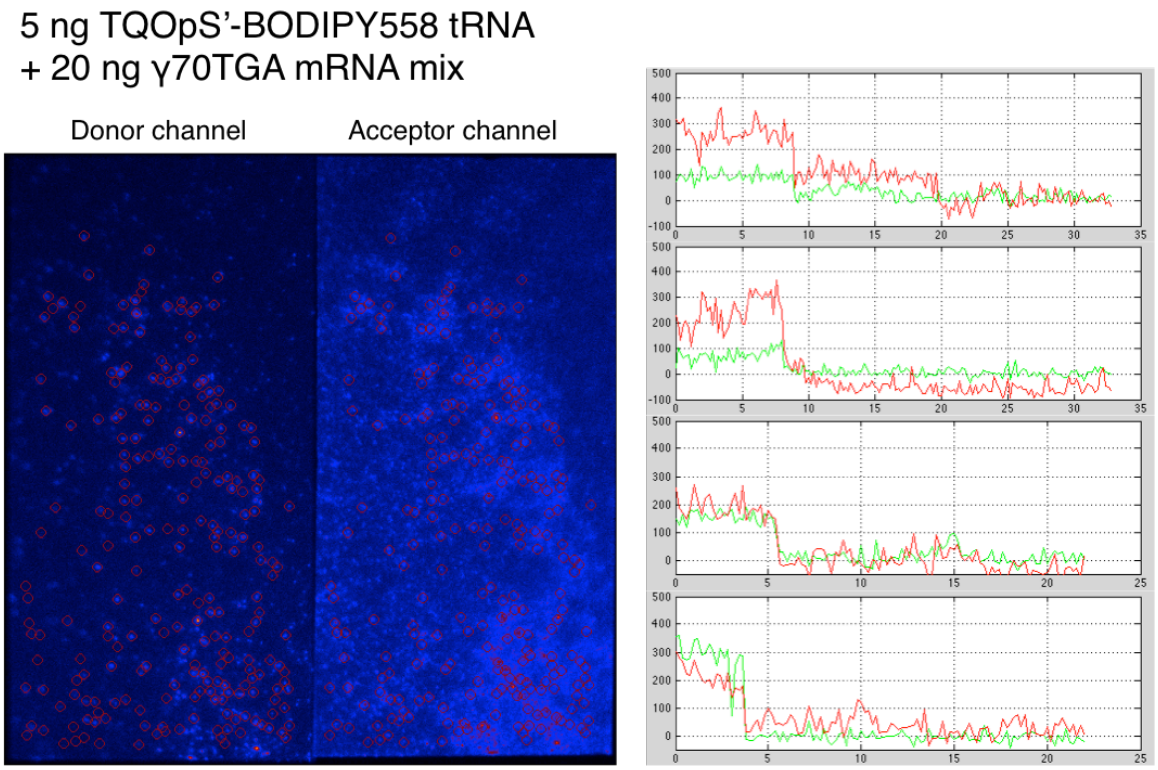

Figure 6.11. Two-color fluorescence image and fluorescence traces from selected puncta of a cell injected with TQOpS'-BODIPY558 tRNA and γ70TGA mRNA mix and labeled with αBtxAlexa488. Puncta recognized by IDL scripts are surrounded by red circles in this image. Entire fluorescence image is shown with the same "heatmap" false-color scheme. Donor channel and acceptor channel represent the same field of view imaged at different emission wavelengths. Fluorescence traces show donor channel intensity (green) and acceptor intensity (red) for the same punctum. Horizontal axis is time (s) and vertical axis is intensity (counts).

Critically, very similar fluorescence traces were seen for puncta from control cells injected with tRNA-BODIPY558 only (no receptor mRNA) (Figure 6.12). For this condition, sparse Alexa488 donor fluorophores are likely present from nonspecific labeling by Alexa488-α-bungarotoxin. High background from BODIPY558 in the acceptor channel raises the possibility of nonspecific spatial overlap of fluorophores. However, fluorescence intensities in the donor and acceptor channels are correlated in many cases, suggesting either specific association of α-bungarotoxin and BODIPY558 (a

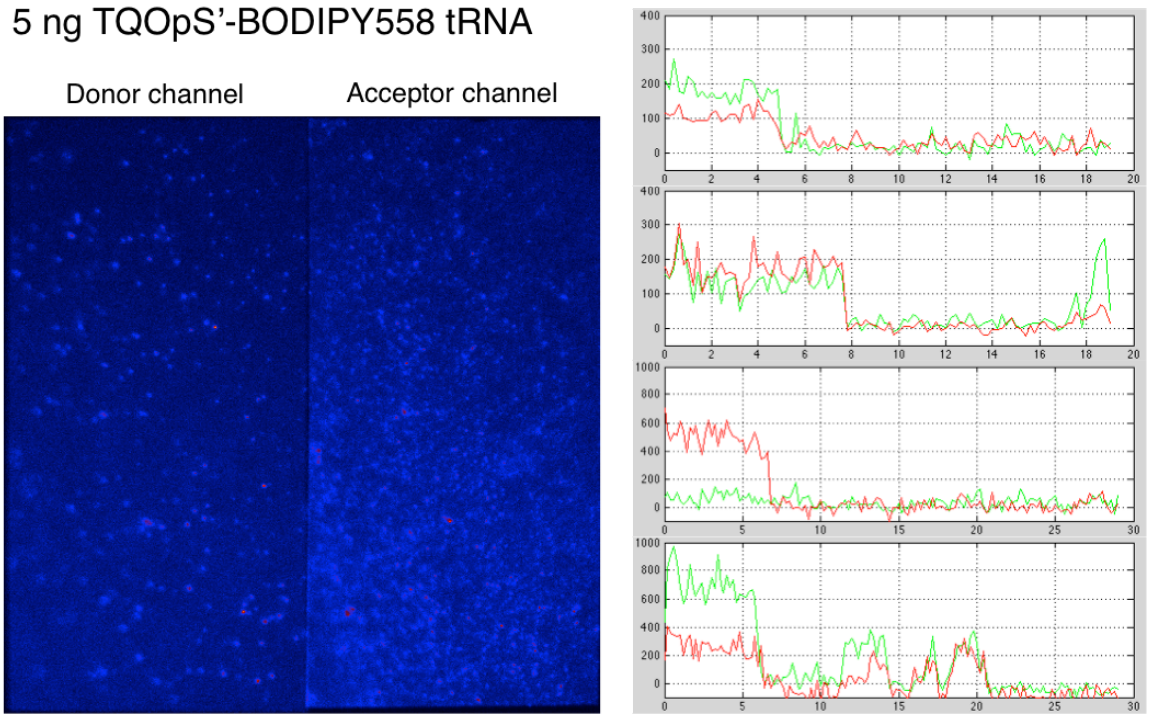

Figure 6.12. Two-color fluorescence image and fluorescence traces from selected puncta of a cell injected with TQOpS'-BODIPY558 tRNA and labeled with αBtxAlexa488. Entire fluorescence image is shown with the same "heatmap" false-color scheme. Donor channel and acceptor channel represent the same field of view imaged at different emission wavelengths. Fluorescence traces show donor channel intensity (green) and acceptor intensity (red) for the same punctum. Horizontal axis is time (s) and vertical axis is intensity (counts).

mechanism for this is unknown) or presence of another species with a broad fluorescence spectrum that spans both wavelength windows (inconsistent with either Alexa488 or BODIPY558). Local "breathing" of the plasma membrane in the vertical plane – in and out of TIRF illumination – is also plausible. Regardless of the origin of this effect, these control results suggest that the γ70TGA mRNA + tRNA-BODIPY558 two-color fluorescence traces cannot be trusted as FRET. Presumably, "background" fluorescence from injected tRNA-BODIPY is once again the issue.

6.3.4 Attempts at fluorophore conjugation by azide-alkyne cycloaddition

In an effort to circumvent the high background fluorescence levels seen from injected tRNA-BODIPY, we attempted dye conjugation to surface-expressed receptors in a labeling step. The desired attributes of labeling were high specificity for the desired nAChR site and low nonspecific labeling of the cell surface. We selected copper-catalyzed azide-alkyne cycloaddition ("click chemistry") as the ligation chemistry, which has extensive precedent for the labeling of biological samples.[23] In the envisioned ligation scheme, the alkyne is incorporated site-specifically into the nAChR as an unnatural amino acid side chain. Propargyl glycine (Pra), which is commercially available, (Figure 6.13A) was chosen and was ligated to tRNA by standard methods. This amino acid was effectively incorporated at the nAChR α70 site (data not shown), which is known to be solvent-accessible.[14]

A principal concern when conducting copper-catalyzed click chemistry *in vivo* is the toxicity of copper to cells. We first sought to assess copper toxicity in our system before actually attempting the coupling reaction since, to our knowledge, copper-

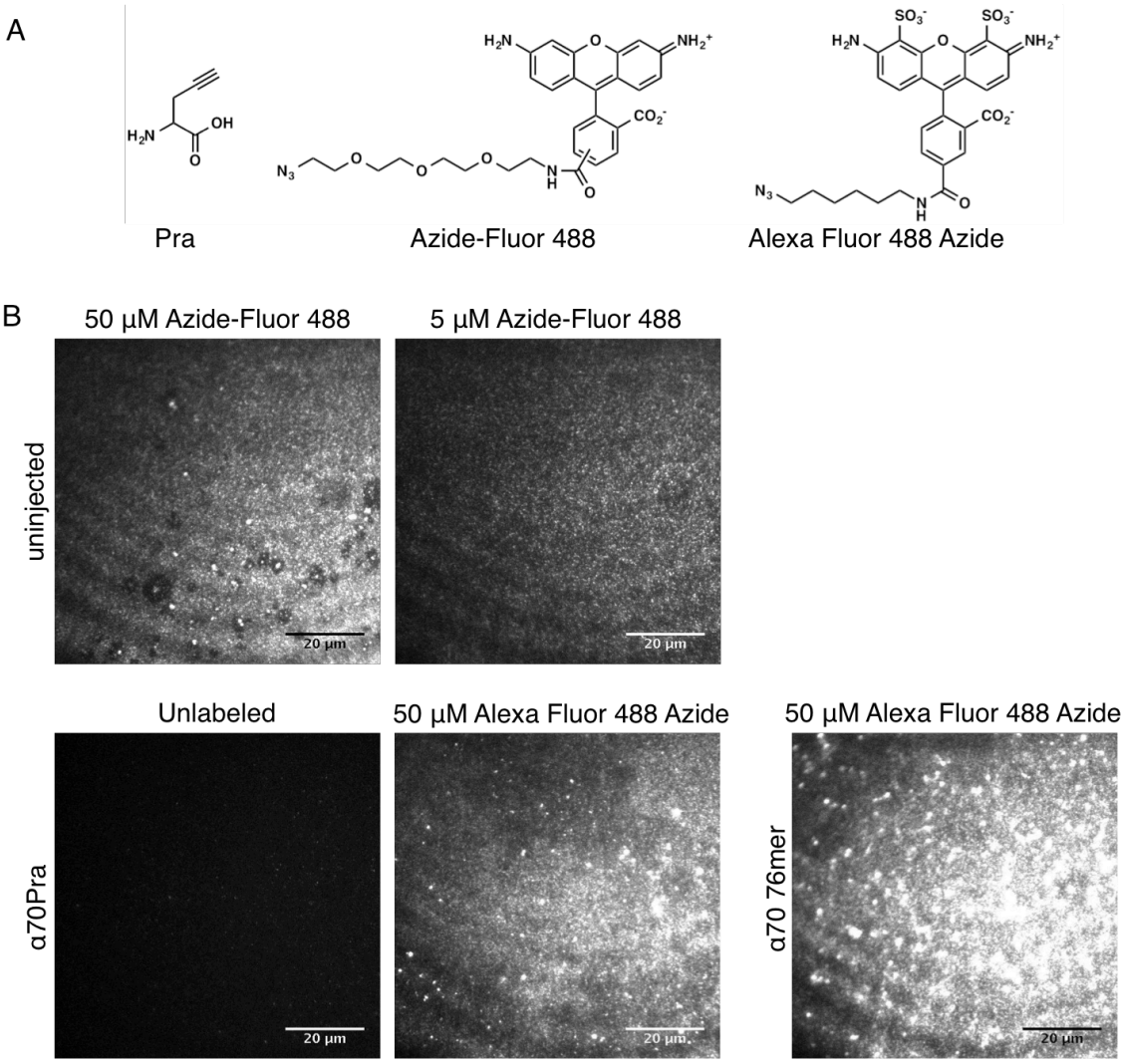

Figure 6.13. (A) Structures of propargyl glycine (Pra), Azide-Fluor 488, and Alexa Fluor 488 Azide. **(B)** TIRF images of oocytes labeled with azido dyes. In the top two panels, oocytes were simply incubated with the azido dye in ND96 solution. In the bottom three panels, oocytes were exposed to copper click conditions (Table 6.1 Condition 1) in the presence of azido dye in ND96.

Table 6.1. Analysis of cell health by whole cell electrophysiology after 1 hr exposure to copper-catalyzed azide-alkyne cycloaddition conditions.

	Untreated	**Condition 1**	**Condition 2**
Additives to ND96 incubation buffer		100 µM $CuSO_4$ 500 µM THPTA 2.5 mM Na Ascorbate	1 mM $CuSO_4$ 500 µM THPTA 2.5 mM Na Ascorbate
Resting potential (mV)	-68 ± 3	-27 ± 1	Cells appear swollen, ~1/3 ruptured after 1 hr (not analyzed by electrophysiology)
Leak Current (mA)	-0.008 ± 0.001	-0.13 ± 0.03	
EC_{50} (µM ACh)	23.9 ± 0.6	27.9 ± 0.6	

catalyzed click chemistry has not been reported on *Xenopus* oocytes. Oocytes expressing the wild type nAChR were exposed to standard click conditions for a typical reaction time of 1 hr (Table 6.1).[24] In these conditions, the copper is supplied as Cu(II), which is reduced to the active Cu(I) species *in situ* by ascorbate in the presence of the tris(3-hydroxypropyltriazolylmethyl)amine (THPTA) copper ligand.[24] While a reduction of the negative membrane resting potential and an increase in the leak current after incubation suggest some reduction in cell health, these cells survived a 40 min series of ACh applications to yield a dose-response curve with an EC_{50} only modestly shifted from wild type. Tenfold higher concentrations of copper, however, result in cell death. These results suggest that cells could still be viable for *in vivo* imaging after exposure to standard copper click conditions, though some reduction in cell health is expected.

Next we assessed the viability of labeling by exposing oocytes to azide-conjugated dyes. We initially selected a commercially available rhodamine-derived azido dye, Azide-Fluor 488 (Figure 6.13A). High fluorescence levels were seen after exposing uninjected oocytes to a standard labeling concentration (50 μM) for 45 min, even after copious washes (5x) with buffer. A tenfold lower concentration of dye (lower than what is ideal for *in vivo* labeling) also gave appreciable levels of fluorescence (Figure 6.13B). We reasoned that a charged, more hydrophilic dye might give less nonspecific labeling, so we tested another commercially available azido dye, AlexaFluor 488-Azide (Figure 6.13B). Unfortunately we also observed high levels of background fluorescence for this dye. Indistinguishable fluorescence levels were seen for α70Pra-expressing cells treated with this dye in a labeling solution (Table 6.1, Condition 1) and for identically treated cells injected with α70TAG mRNA and unacylated 76mer tRNA

(Figure 6.13B). We conclude that these azido dyes give unacceptably high levels of nonspecific labeling to be viable in this system.

6.3.5 Design and synthesis of a fluorescence-quenched tRNA

Pursing the original scheme of fluorophore incorporation by nonsense suppression, we sought an alternative approach to reduce high background fluorescence from injected fluorescent tRNA. We reasoned that we might modify the tRNA-BODIPY in such a way that the BODIPY's fluorescence was quenched until the dye is incorporated into the protein of interest. Toward this end, we employed a "dark quencher" – a molecule that efficiently dissipates energy nonradiatively, and in this application acts as a FRET acceptor for a donor fluorophore.[25]

Positioning of this quencher on the tRNA is expected to be critical: it must be in sufficiently close proximity to the BODIPY fluorophore at the tRNA's 3' terminus to efficiently quench its fluorescence, yet it must be in a position tolerated by the ribosome during translation. We reasoned that the 5' terminus of the tRNA was a sensible site for quencher incorporation, allowing for relatively facile quencher incorporation and close proximity to BODIPY (Figure 6.14). Tolerance of a large structural modification to this region was largely unexplored, but at least modest changes are tolerated: removal of a native tRNA's 5' phosphate has a small effect on the rate of translation,[26] and we routinely use suppressor tRNAs bearing an unnatural 5' triphosphate.[27]

The Iowa Black FQ quencher, a dark quencher available from Integrated DNA Technologies, was selected for these experiments. The structure of this quencher has not been released by the manufacturer, but it is reported to have a molecular weight of 442.4

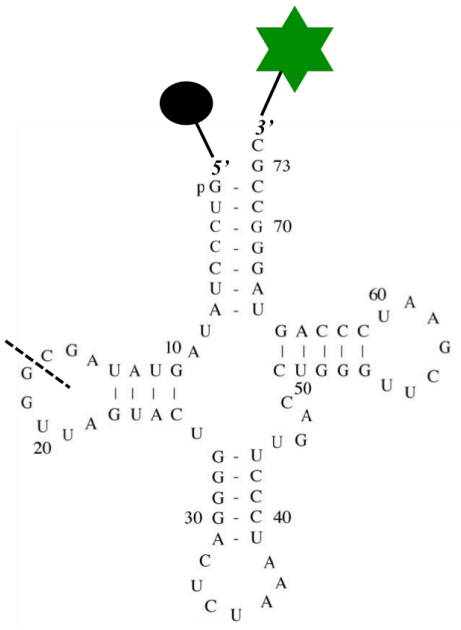

Figure 6.14. Schematic of Q-TQAS-BODIPYFL quenched fluorescent tRNA. Dashed line: disconnection of 16mer and 57mer component fragments. Black oval: Iowa Black FQ dark quencher. Green star: Lys-BODIPYFL.

g/mol and an absorbance maximum at 531 nm, which is appropriate for good spectral overlap with BODIPYFL fluorescence emission. To assemble a tRNA bearing this quencher group, we obtained a custom 16mer oligoribonucleotide corresponding to the first 16 bases of the TQAS suppressor tRNA's 5' terminus with the Iowa Black FQ quencher appended to it's 5' end (Integrated DNA Technologies). This oligo was then ligated to a transcribed 57mer oligo comprising the remainder of TQAS, minus the final two 3' nucleotides, to yield the quencher-tagged "74mer." Prior to the ligation, the 57mer was treated with phosphatase to remove its 5' triphosphate, then treated with polynucleotide kinase to add a single 5' phosphate, rendering this oligo competent for ligation to the 16mer by T4 RNA ligase. The ligation product was purified by preparative polyacrylamide gel electrophoresis (PAGE). This "74mer" could then be ligated to aminoacylated dCA by standard methods.[27] In this fashion, full length "76mer"

TQAS tRNA bearing a 5’ Iowa Black FQ quencher and acylated at its 3’ end with Lys-BODIPYFL (Q-TQAS-BODIPYFL) was prepared, as was 76mer tRNA bearing a 5’ quencher, but no 3’ amino acid (Q-TQAS 76mer) for use in control experiments. Identity of the products was confirmed by MALDI-MS and also by UV-Vis absorption spectra (Figure 6.15). These spectra confirm that the Iowa Black FQ quencher absorbance should have good spectral overlap with BODIPYFL emission (~515 – 560 nm).

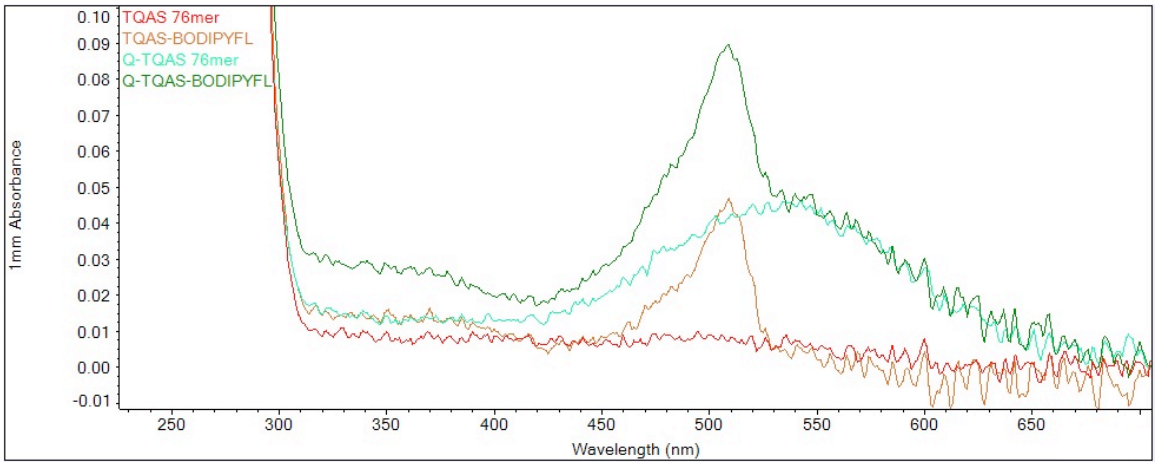

Figure 6.15. UV-Vis spectra of tRNAs

Next we sought to assess the translational competence of tRNA bearing a 5’ quencher. Q-TQAS-BODIPYFL tRNA was evaluated for nonsense suppression at the β70 site. Encouragingly, we observed appreciable expression of receptors by electrophysiology when using this tRNA, though the expression level was reduced relative to the condition for regular TQAS-BODIPYFL tRNA lacking the quencher (Figure 6.16). Q-TQAS 76mer conditions showed significantly less expression than those for acylated tRNA, suggesting that reacylation still low for tRNA with a 5’

quencher. In another experiment, we observed that Q-TQAS-Trp tRNA was competent for tryptophan incorporation by nonsense suppression at the αW149 site (data not shown).

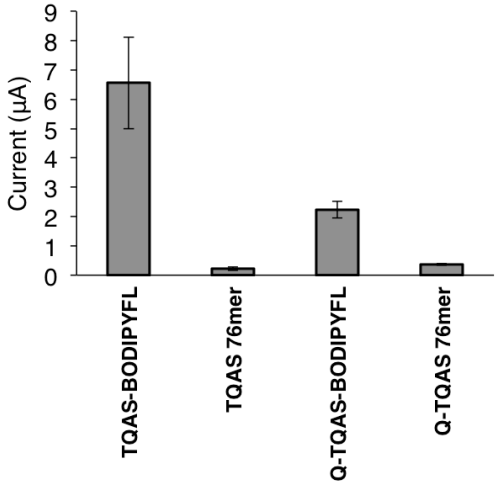

Figure 6.16. Maximal whole cell currents from cells injected with 10 ng β70TAG nAChR mRNA mix and 10 ng of the specified tRNA. Cells were incubated for 24 hrs after injection and assayed with a saturating concentration of ACh (1000 μM).

Table 6.2. tRNA fluorescence readings. All samples are 16 μM in 1 mM NaOAc buffer (pH 4.5). Fluorescence readings were taken on 5 μL samples using the Flexstation III fluorescent plate reader with excitation at 485 nm and emission filtered to 520 nm.

	520 nm fluorescence (RFU)
Buffer	0.413
TQAS-BODIPYFL	1840
Q-TQAS-BODIPYFL	512
TQAS 76mer	2.33
Q-TQAS 76mer	0.531

The efficiency of fluorescence quenching by Iowa Black FQ on the Q-TQAS-BODIPYFL tRNA was assessed using the Flexstation III fluorescent plate reader. We measured BODIPYFL fluorescence for tRNA samples and observed a 72% reduction in fluorescence for Q-TQAS-BODIPYFL relative to TQAS-BODIPYFL (Table 6.2). These

results do suggest fluorescence quenching of BODIPYFL by Iowa Black FQ on the tRNA, though appreciable fluorescence remains. To confirm that fluorescent impurities were not present (for example, RNAs with BODIPY but lacking the quencher), we performed fluorescence imaging of tRNA samples run out on a denaturing PAGE gel (Figure 6.17). For both TQAS-BODIPYFL and Q-TQAS-BODIPYFL tRNAs, we see only a single fluorescent species with emission at BODIPYFL wavelengths (515-545 nm), consistent with the anticipated tRNA species. Ethidium bromide staining allows for visualization of all nucleic acid species using a distinct fluorescence window (560-580 nm). This fluorescence window indicates multiple RNA species in both of these samples, which may account for hydrolysis of Lys-BODIPYFL off of the tRNA (this species is seen as a minor product by MALDI-MS). However, imaging of this gel suggests that there are not any other fluorescent species present in the sample that would account for "unquenched" fluorescence from Q-TQAS-BODIPYFL.

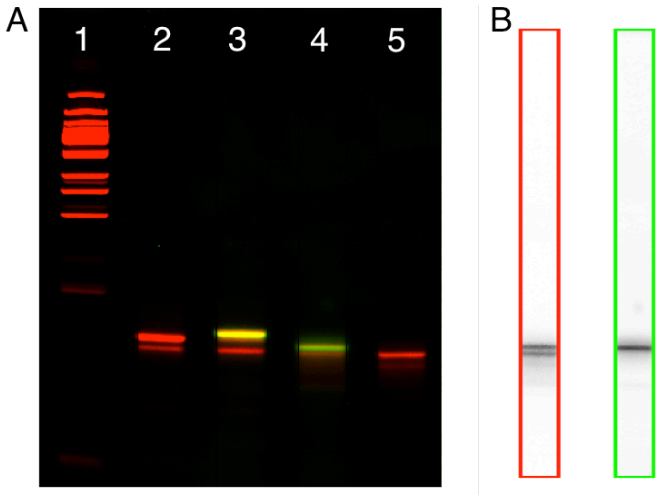

Figure 6.17. (A) Fluorescence image of an ethidium bromide-stained denaturing polyacrylamide gel of tRNA species. Lanes: (1) 50 bp DNA ladder; (2) TQAS 76mer; (3) TQAS-BODIPYFL; (4) Q-TQAS-BODIPYFL; (5) Q-TQAS 76mer. 0.2 µg RNA was loaded into each lane. Green false color is BODIPYFL fluorescence (515-545 nm) and red false color is ethidium bromide fluorescence (560-580 nm). **(B)** Ethidium bromide fluorescence channel (red border) and BODIPYFL fluorescence channel (green border) for Q-TQAS-BODIPYFL (Lane 4).

It is plausible that the quencher and BODIPY are too distant from each other on the tRNA for highly efficient quenching. In a representative tRNA (yeast Phe), the 5' phosphate and 3' hydroxyl groups are 24 Å distant from each other.[28] The 5' quencher and 3' BODIPY fluorophore will be more distant still – perhaps another 10 – 15 Å, if the Lys side chain and (unknown) quencher tether are included. The Förster radius of the BODIPYFL/Iowa Black FQ pair has not been reported, though it is plausible that at the ~25-40 Å separation of the BODIPY and Iowa Black on the tRNA, quenching by FRET may be in the 70% range suggested by our fluorescence measurements (Table 6.2).

Finally, we imaged oocytes injected with Q-TQAS-BODIPYFL. These oocytes were devitellinized by the standard manual method. At standard injection amounts (10 ng tRNA), we observed high levels of fluorescence for the tRNA-only condition and no discernible difference in fluorescence for tRNA + β70TAG mRNA (Figure 6.18A). Hence the original aim of the quenched tRNA to reduce background fluorescence levels to the extent that receptors can be distinguished from background has not been met. We also imaged cells injected with far less tRNA (0.2 ng) such that (background) fluorescence would be sparse and punctate. Again, we saw comparable levels of fluorescence (now punctate) for conditions with and without receptor mRNA (Figure 6.18B). Investigation of individual puncta brightness revealed similar values whether the cells were injected with Q-TQAS-BODIPYFL or TQAS-BODIPYFL (~3000 - 4000 counts). This is surprising, given the 72% reduction in bulk fluorescence measured for the quencher-bearing tRNA (Table 6.2). One explanation could be high levels of Lys-BODIPYFL hydrolysis off of the tRNA or some other form of tRNA degradation that liberates BODIPY from the quencher.

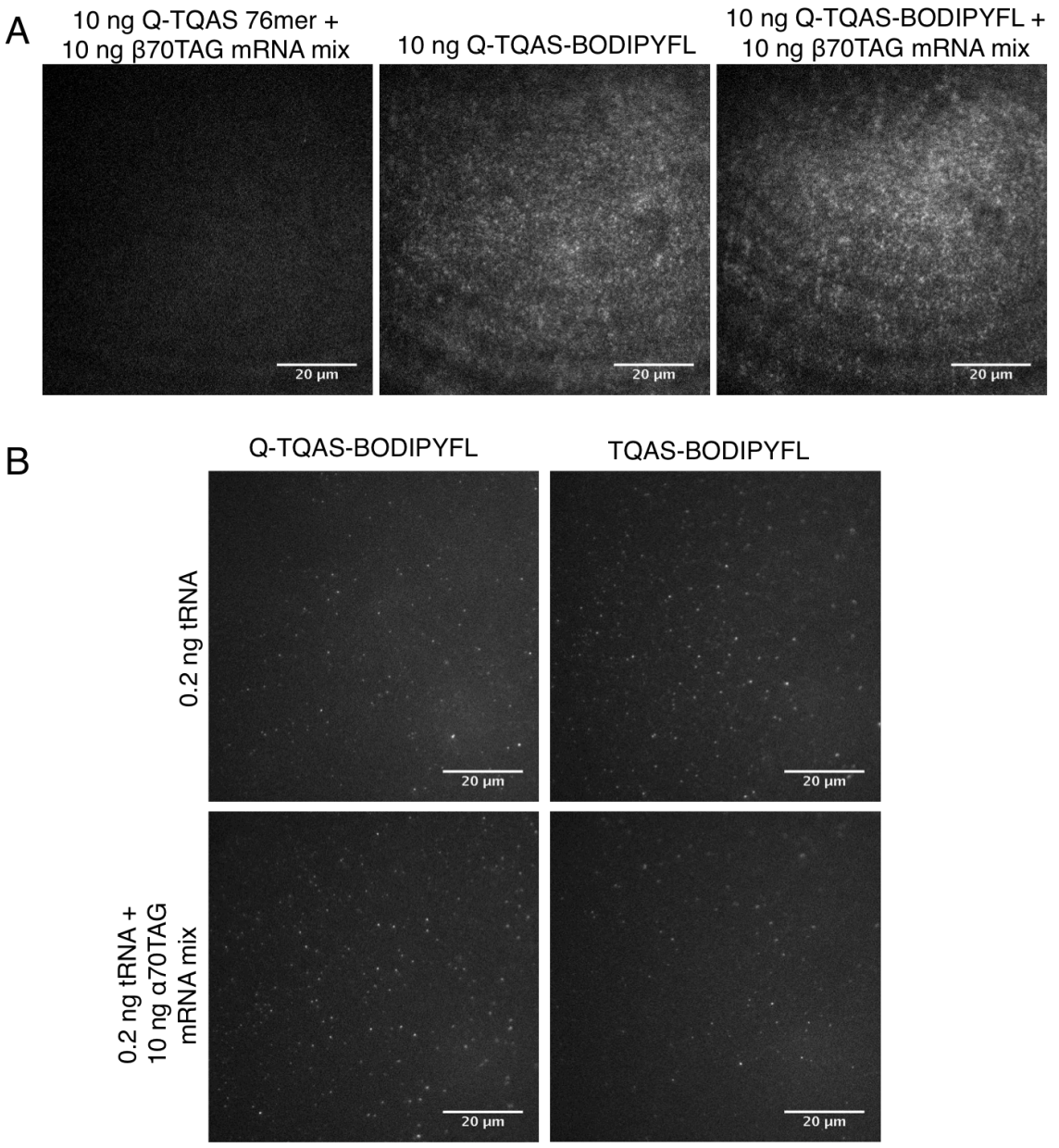

Figure 6.18. TIRF images of oocytes injected with fluorescence-quenched tRNA. **(A)** Q-TQAS-BODIPY tRNA still gives appreciable levels of background fluorescence. Brightness range: 400 counts (black) to 2000 counts (white). **(B)** TIRF images of cells injected with low amounts of tRNA. Puncta from all conditions have comparable brightness (~3000 – 4000 counts). Image brightness range: 100 counts (black) to 4500 counts (white).

6.4 Conclusions

Despite various efforts to circumvent background fluorescence from injected tRNA, we were unable to identify conditions in which fluorescent receptors could be visualized above background. Background fluorescence will be an inherent issue for *in vivo* imaging with fluorophore incorporation by nonsense suppression. TIRF microscopy offers a reduction of intracellular fluorescence seen, but in the experiments described in this chapter, background fluorescence, apparently at or near the glass surface, was still unmanageably high.

For future efforts on this project, several areas seem promising for improvements. First, clean plasma membrane preparation will likely be facilitated by only selecting cells of excellent health and by taking special care to use meticulous manual devitellinization technique. Second, dyes other than BODIPY that have greater photostability could be explored. A literature search revealed no studies using BODIPY dyes for single molecule FRET, likely due to the their limited photostability. Cy3 and Cy5 are the most widely used FRET pair for single molecule imaging,[29] and could be viable alternatives to BODIPY, though their slightly larger size could limit the efficiency of their incorporation into proteins by nonsense suppression. Finally, click chemistry conjugation of dyes could be viable using recently developed "turn on" fluorophores whose fluorescence intensity increases dramatically upon conjugation. This could offer a work-around for the high levels of nonspecific dye labeling observed in the fluorophore conjugation attempts described above.

6.5 Experimental

6.5.1 Molecular biology and in vivo *expression*

Nonsense suppression was performed using techniques described previously on the mouse muscle embryonic nAChR, $(\alpha 1)_2\beta 1\gamma\delta$, in the pAMV vector.[30] Stage V-VI *Xenopus laevis* oocytes were injected with 1 ng total mRNA in a 2:1:1:1 ratio of α1:β1:γ:δ for wild-type experiments. For nonsense suppression experiments, oocytes were typically injected with 10 ng tRNA and 10 ng total mRNA in a 10:1:1:1 ratio of α1:β1:γ:δ for suppression in the α subunit, in a 2:5:1:1 ratio for suppression in the β subunit, or in a 2:1:5:1 ratio for suppression in the γ subunit. tRNAs bearing a 6-nitroveratryloxycarbonyl protecting group were deprotected prior to injection via irradiation with a 500 W Hg/Xe arc lamp, filtered with WG-334 and UG-11 filters prior to injection. Deprotection was carried out for 4 min only to limit the amount of BODIPY photobleaching.[12] Oocytes were injected for 24-48 hrs prior to imaging or electrophysiology.

6.5.2 Electrophysiology

Electrophysiology recordings were performed using the OpusXpress 6000A (Axon Instruments) at a holding potential of −60 mV. The running buffer was a Ca^{2+} free ND96 solution (96 mM NaCl, 2 mM KCl, 1 mM $MgCl_2$, and 5 mM HEPES, pH 7.5). Agonist doses in Ca^{2+}-free ND96 were applied for 15 s followed by a 116 s wash with the running buffer. Dose-response relations were fit to the Hill equation to obtain EC_{50} and Hill coefficient values, which are reported as averages ± standard error of the fit.

6.5.3 Oocyte membrane preparation

The oocyte vitelline membrane was removed prior to imaging. Under standard

conditions (used unless specified otherwise), oocytes were incubated in hypertonic media (220 mM Na aspartate, 10 mM EDTA, 2 mM $MgCl_2$, and 10 mM HEPES, pH 7.4) for 5–15 min. Under a dissecting microscope, the vitelline membrane, which was visible over the underlying plasma membrane, was manually removed using forceps. In one alternative condition,[19] cells are incubated in ND96 solution containing 4 mg/mL collagenase (Sigma, Type IA) and 4 mg/mL hyaluronidase (Sigma, Type IV-S) for 60 min, after which cells are exposed to hypertonic media and manually stripped of their vitelline membrane, as described above. In another alternative condition,[20] complete digestion of the vitelline membrane is achieved by protease treatment (0.05 mg/mL in ND96, Type VIII, Sigma) with gentle shaking for 30 min. Digestion of the vitelline membrane is visualized under light microscopy. After any devitellinization procedure, the oocyte is immediately transferred to a glass-bottom petri dish (MatTek) for TIRF imaging. Oocytes were typically placed on the dish with their animal pole facing down, as the vegetal pole generally shows higher autofluorescence.

6.5.4 Total internal reflection fluorescence (TIRF) imaging

TIRF microscopy was conducted on an Olympus IX81 inverted microscope. A JDS Uniphase 2219 488 nm argon ion laser was coupled to the microscope via a fiber optic. Through-objective TIRF imaging was conducted using an Olympus 100x 1.45-NA objective lens. Images were captured using an Andor iXon 897 electron-multiplying charge coupled device (EMCCD) camera. Typical image integration time was 0.2 s. Andor iQ2 software was used to acquire the data, which were analyzed using ImageJ (National Institutes of Health). A region of interest on the cell was selected to establish

focus on the membrane and the TIRF condition. Imaging was conducted elsewhere on the cell, to limit the effect of photobleaching on measurements.

6.5.5 Azido dye labeling under copper-catalyzed click conditions

In tests to assess cell viability under conditions for copper-catalyzed azide-alkyne cycloaddition, *Xenopus* oocytes were exposed to a solution of ND96 buffer containing 100 μM $CuSO_4$, 500 μM tris(3-hydroxypropyltriazolylmethyl)amine ligand (a gift from Lan Ban, Hsieh-Wilson lab, Caltech), and 2.5 mM sodium ascorbate. For labeling attempts using an azido dye conjugate, oocytes were incubated in the above solution additionally containing 50 μM azido dye (either Azide-Fluor 488 [Click Chemistry Tools] or AlexaFluor 488-Azide [Life Technologies]) for 45 – 60 min. Next cells were rinsed three times with ND96 buffer, incubated in ND96 for 15 min, rinsed again with ND96, and finally incubated another 15 min in ND96. Cells were then devitellinized using the standard manual devitellinization method and imaged.

6.5.6 Two-color TIRF imaging and image analysis

For all two-color TIRF imaging experiments, cells expressing the appropriate receptors of interest were labeled with Alexa488-labeled α-bungarotoxin (αBtxAlexa488, Life Technologies). Cells were incubated in 20 nM αBtxAlexa488 for 6.5 hrs at 18°C, then rinsed twice with ND96, incubated in 5 mg/mL BSA in ND96 for 10 min, then rinsed with ND96 and incubated for 30 min and rinsed again with ND96 and incubated for 30 min. Cells were then devitellinized using the standard manual devitellinization method and imaged.

For these experiments, an Optosplit II (Cairn Research) beam splitter was installed in the fluorescence emission light path directly in front of the camera. In our configuration of this device, incident light is split by a 560 nm dichroic mirror. Reflected light ("donor channel") passes through a 500-550 nm bandpass filter and transmitted light ("acceptor channel") passes through a 575-615 nm bandpass filter. These paths are focused side-by-side on the camera. In our experiments, intensity of the donor channel was significantly higher than intensity of the acceptor channel, so a neutral density filter was placed in the donor channel path.

IDL scripts written by Taekjip Ha's lab at the University of Illinois were used for single puncta data analysis.[31] Using a MATLAB script, TIFF files obtained from the Andor iQ2 acquisition software were converted to PMA files for further analysis. In order to correlate puncta in the donor channel to corresponding puncta in the acceptor channel, a mapping file was created using images of fluorescent beads collected on our TIRF microscope in two-color mode. The beads (Duke Scientific G100 green fluorescent beads) were sparsely distributed on a glass bottom dish identical to those used for oocyte imaging and a new mapping file was created for each imaging session, in case of variation in optical alignment of the two channels. This mapping file was applied to the actual movies of interest and fluorescence traces for each punctum identified by the script were extracted from both donor and acceptor channels. These traces were analyzed and plotted in MATLAB.

6.5.7 tRNA synthesis and characterization

TQAS-BODIPYFL and TQAS-BODIPY558 tRNAs were synthesized by standard methods, ligating dCA-Lys-BODIPYFL or dCA-Lys-BODIPY558 to 74mer TQAS.[27]

dCA-Lys-BODIPYFL and dCA-Lys-BODIPY558 were prepared by Walrati Limapichat.[12]

Q-TQAS-BODIPYFL tRNA was synthesized by ligation of a transcribed 57mer oligoribonucleotide (3' portion) to a 16mer oligoribonucleotide (5' portion) to yield "74mer" TQAS tRNA. The 16mer oligoribonucleotide GUCCCUAUAGUAUAGC (all sequences are written 5' to 3') with a Iowa Black FQ quencher appended to its 5' terminus was purchased from Integrated DNA Technologies. The 57mer of the sequence GGUUAGUACUGGGGACUCUAAAUCCCUUGACCUGGGUUCGAAUCCCAGUA GGGCCGC was prepared by runoff transcription of a modified DNA oligonucleotide bearing 2' OMe groups on its two terminal 5' nucleotides. To render the 57mer competent for ligation to the 16mer, its 5' triphosphate was removed using calf intestinal alkaline phosphatase (New England Biolabs), with purification by PCI extraction. The resulting product was treated with T4 polynucleotide kinase (New England Biolabs), with purification by PCI extraction, to yield the desired 57mer with a 5' monophosphate. 16mer and 57mer were ligated to each other using T4 RNA ligase 1 (New England Biolabs). 16mer and 57mer were mixed in a 2:1 molar ratio, annealed by heating to 90°C for 2 min and then cooling to room temperature, and then subjected to standard T4 RNA ligase ligation conditions.[27] The crude product of the ligation reaction was isolated by PCI extraction. This product was purified by preparative acrylamide gel electrophoresis (PAGE) on a denaturing TBE 15% urea gel (Life Technologies). Finally, the "74mer" oligonucleotide was ligated to dCA-Lys-BODIPYFL by standard methods[27] to yield Q-TQAS-BODIPYFL tRNA. Control unacylated Q-TQAS 76mer tRNA was synthesized by ligating the 74mer to unacylated dCA. The identity of RNA products throughout the

synthesis was confirmed by matrix-assisted laser desorption-ionization time-of-flight mass spectrometry on a 3-hydroxypicolinic acid matrix. Final tRNA products were also characterized by UV-Vis on a Nanodrop 2000 spectrophotometer (Thermo Scientific).

Final tRNA products were also characterized by denaturing PAGE on a 15% TBE urea gel (Life Technologies). 0.2 μg of each tRNA was loaded onto the gel, which was stained with ethidium bromide after running. The gel was imaged on a Typhoon FLA 9000 imager (GE Healthcare Life Sciences) both at 473 nm excitation with a 515-545 nm bandpass emission filter and at 532 nm excitation with a 560-580 nm bandpass emission filter.

6.6 References

1. Dacosta, C. J. B. & Baenziger, J. E. Gating of pentameric ligand-gated ion channels: structural insights and ambiguities. *Structure* **21,** 1271–1283 (2013).
2. Taly, A. *et al.* Normal mode analysis suggests a quaternary twist model for the nicotinic receptor gating mechanism. *Biophys J* **88,** 3954–3965 (2005).
3. Hilf, R. J. C. & Dutzler, R. Structure of a potentially open state of a proton-activated pentameric ligand-gated ion channel. *Nature* **457,** 115–118 (2009).
4. Bocquet, N. *et al.* X-ray structure of a pentameric ligand-gated ion channel in an apparently open conformation. *Nature* **457,** 111–114 (2009).
5. Hilf, R. J. C. & Dutzler, R. X-ray structure of a prokaryotic pentameric ligand-gated ion channel. *Nature* **452,** 375–379 (2008).
6. Unwin, N. & Fujiyoshi, Y. Gating movement of acetylcholine receptor caught by plunge-freezing. *J Mol Biol* **422,** 617–634 (2012).
7. Kalstrup, T. & Blunck, R. Dynamics of internal pore opening in K(V) channels probed by a fluorescent unnatural amino acid. *Proc. Natl. Acad. Sci. U.S.A.* **110,** 8272–8277 (2013).
8. Turcatti, G. *et al.* Probing the structure and function of the tachykinin neurokinin-2 receptor through biosynthetic incorporation of fluorescent amino acids at specific sites. *J. Biol. Chem.* **271,** 19991–19998 (1996).
9. Pantoja, R., Rodriguez, E. A., Dibas, M. I., Dougherty, D. A. & Lester, H. A. Single-molecule imaging of a fluorescent unnatural amino acid incorporated into nicotinic receptors. *Biophys J* **96,** 226–237 (2009).
10. Ceriotti, A. & Colman, A. Protein transport from endoplasmic reticulum to the

Golgi complex can occur during meiotic metaphase in Xenopus oocytes. *J. Cell Biol.* **109,** 1439–1444 (1989).

11. Rodriguez, E. A., Lester, H. A. & Dougherty, D. A. In vivo incorporation of multiple unnatural amino acids through nonsense and frameshift suppression. *Proceedings of the National Academy of Sciences* **103,** 8650–8655 (2006).
12. Limapichat, W. in (Dougherty, D. A.) 1–220 (California Institute of Technology, 2012).
13. Kajihara, D. *et al.* FRET analysis of protein conformational change through position-specific incorporation of fluorescent amino acids. *Nat Methods* **3,** 923–929 (2006).
14. Gallivan, J. P., Lester, H. A. & Dougherty, D. A. Site-specific incorporation of biotinylated amino acids to identify surface-exposed residues in integral membrane proteins. *Chemistry & biology* **4,** 739–749 (1997).
15. Rodriguez, E. A., Lester, H. A. & Dougherty, D. A. Improved amber and opal suppressor tRNAs for incorporation of unnatural amino acids in vivo. Part 1: Minimizing misacylation. *Rna* **13,** 1703–1714 (2007).
16. Panchuk-Voloshina, N. *et al.* Alexa dyes, a series of new fluorescent dyes that yield exceptionally bright, photostable conjugates. *The journal of histochemistry and cytochemistry : official journal of the Histochemistry Society* **47,** 1179–1188 (1999).
17. Larabell, C. A. & Chandler, D. E. The extracellular matrix of Xenopus laevis eggs: a quick-freeze, deep-etch analysis of its modification at fertilization. *J. Cell Biol.* **107,** 731–741 (1988).
18. Sonnleitner, A., Mannuzzu, L. M., Terakawa, S. & Isacoff, E. Y. Structural rearrangements in single ion channels detected optically in living cells. *Proceedings of the National Academy of Sciences* **99,** 12759–12764 (2002).
19. Choe, H. & Sackin, H. Improved preparation of Xenopus oocytes for patch-clamp recording. *Pflugers Arch* **433,** 648–652 (1997).
20. Wang, M. H. A technical consideration concerning the removal of oocyte vitelline membranes for patch clamp recording. *Biochemical and Biophysical Research Communications* **324,** 971–972 (2004).
21. Rodriguez, E. A., Lester, H. A. & Dougherty, D. A. Improved amber and opal suppressor tRNAs for incorporation of unnatural amino acids in vivo. Part 2: evaluating suppression efficiency. *Rna* **13,** 1715–1722 (2007).
22. Unwin, N. Refined structure of the nicotinic acetylcholine receptor at 4A resolution. *Journal of Molecular Biology* **346,** 967–989 (2005).
23. Sletten, E. M. & Bertozzi, C. R. Bioorthogonal Chemistry: Fishing for Selectivity in a Sea of Functionality. *Angew. Chem. Int. Ed.* **48,** 6974–6998 (2009).
24. Hong, V., Presolski, S. I., Ma, C. & Finn, M. G. Analysis and optimization of copper-catalyzed azide-alkyne cycloaddition for bioconjugation. *Angew. Chem. Int. Ed. Engl.* **48,** 9879–9883 (2009).
25. Silverman, A. P. & Kool, E. T. Quenched probes for highly specific detection of cellular RNAs. *Trends in Biotechnology* **23,** 225–230 (2005).
26. Sprinzl, M. & Graeser, E. Role of the 5'-terminal phosphate of tRNA for its function during protein biosynthesis elongation cycle. *Nucleic Acids Res* **8,** 4737–4744 (1980).

27. Nowak, M. W. *et al.* In vivo incorporation of unnatural amino acids into ion channels in Xenopus oocyte expression system. *Meth. Enzymol.* **293,** 504–529 (1998).
28. Westhof, E. & Sundaralingam, M. Restrained refinement of the monoclinic form of yeast phenylalanine transfer RNA. Temperature factors and dynamics, coordinated waters, and base-pair propeller twist angles. *Biochemistry* **25,** 4868–4878 (1986).
29. Roy, R., Hohng, S. & Ha, T. A practical guide to single-molecule FRET. *Nat Meth* **5,** 507–516 (2008).
30. Xiu, X., Puskar, N. L., Shanata, J. A., Lester, H. A. & Dougherty, D. A. Nicotine binding to brain receptors requires a strong cation-π interaction. *Nature* **458,** 534–537 (2009).
31. Joo, C. & Ha, T. Single-molecule FRET with total internal reflection microscopy. *Cold Spring Harb Protoc* **2012,** (2012).